Malaysian Journal of Chemistry, 2024, Vol. 26(5), 23-33
(Special Issue: *3rd Virtual International Symposium on Sciences 2023*)

Photocatalytic Degradation of Phenol using Copper-Doped Graphitic Carbon Nitride under Fluorescent and Sunlight Irradiation

Nurul Izzah Norhisan[1], Siti Hajar Alias[1]*, Nur Nazzatul Azzin Ahmad Tarmizi[1], Siti Nor Atika Baharin[1], Salman Al Faridzy Akbar[2], Sheikh Ahmad Izaddin Sheikh Mohd Ghazali[3] and Hadi Nur[4]

[1]Advanced Material for Environmental Remediation (AMER) Research Group, School of Chemistry and Environment, Faculty of Applied Sciences, Universiti Teknologi MARA Cawangan Negeri Sembilan, Kampus Kuala Pilah, 72000 Kuala Pilah, Negeri Sembilan, Malaysia

[2]Department of Chemistry, Faculty of Mathematics and Natural Sciences, Universitas Islam Indonesia, Kampus Terpadu UII, Jl. Kaliurang Km 14, Sleman, Yogyakarta, Indonesia

[3]Material, Inorganic, and Oleochemistry (MaterInoleo) Research Group, School of Chemistry and Environment, Faculty of Applied Sciences, Universiti Teknologi MARA Cawangan Negeri Sembilan, Kampus Kuala Pilah, 72000 Kuala Pilah, Negeri Sembilan, Malaysia

[4]Center of Advanced Materials for Renewable Energy (CAMRY), Universitas Negeri Malang, Malang 65145, Indonesia

*Corresponding author (e-mail: sitihajar404@uitm.edu.my)

Phenol is one of the toxic chemicals that can cause water pollution in Malaysia. It can be degraded using a photocatalyst such as graphitic carbon nitride, g-C_3N_4, which has an appropriate band gap for low-energy activation. Nonetheless, g-C_3N_4 has low photocatalytic activity due to the fast charge carrier recombination and low surface area. However, g-C_3N_4 can be doped with metal such as copper to increase the photocatalytic performance in degrading phenol. Therefore, this research aims to evaluate the photocatalytic efficiency of synthesized pure g-C_3N_4 and copper-doped g-C_3N_4 (Cu/g-C_3N_4) for the degradation of phenol under fluorescent and sunlight irradiation. Pure g-C_3N_4 and Cu/g-C_3N_4 were synthesized using the thermal decomposition of melamine and the liquid exfoliation method and characterized using FTIR, XRD, FESEM and EDX. The FTIR confirmed the presence of all vibration peaks of g-C_3N_4. The XRD patterns show that the copper-doped has no significant influence on the structure of pure g-C_3N_4, while the EDX analysis shows the presence of copper in g-C_3N_4. The phenol was treated under fluorescent and sunlight irradiation in the presence of a synthesized photocatalyst. The degradation efficiencies of phenol using 0.5Cu/g-C_3N_4 under the fluorescent light irradiation was 50.76%, while under sunlight irradiation, the degradation efficiency was 55.38% for 120 minutes. The results show the potential of Cu/g-C_3N_4 as a photocatalyst for phenol degradation under visible light irradiation. This study can contribute to the solution of how to address pollution and protect the water ecosystem.

Keywords: Copper doped; graphitic carbon nitride; photocatalytic activity; degradation of phenol

Received: October 2023; Accepted: February 2024

Industries and factories, in general, are frequently linked to environmental problems. Environmental systems can easily be harmed by chemical pollution and cause secondary pollutants to arise as a result of reactions with other reagents and may also produce volatile gases. Other than benzene, alcohol, and other compounds, phenol is one of the substances that can be categorized as harmful chemical pollutants [1]. Phenol is one of the chemical or organic compounds often used in many industries, such as oil refining, plastics manufacturing, petrochemicals, and others, that can result in water pollution. Phenol is high in toxicity and is volatile. A small amount of it can affect the smell and taste of water, which can have a negative effect on human health [2]. In their research, Mei et al. [3] stated that phenol can impact pregnant women, resulting in low-birth-weight kids to preterm delivery. This is because phenol could disrupt the placenta and decrease the baby's development during pregnancy. According to Ismanto et al. [4], phenol is labelled as an anthropogenic Endocrine Disrupting Chemical (EDC). Anthropogenic EDCs are a combination of materials that could affect human health, especially the function of the endocrine system. Disruption to the human endocrine system can increase the possibility of diabetes, thyroid illness, obesity, and other severe diseases.

To tackle this issue, phenol must be degraded to reduce pollution, especially in wastewater. However, the degradation of phenol is limited because the process is complex and require high energy consumption. It

†Paper presented at the 3rd Virtual International Symposium on Sciences (3rd VISoS 2023)

also requires a lot of maintenance, although there are several types of degradation techniques that can be applied [5]. Nevertheless, the ideal approach for phenol degradation is photocatalysis. According to Ameta et al. [6], photocatalysis is a chemical reaction that takes place by a semiconductor and utilizes lights. Oxidation and reduction processes are also reactions that help in the degradation of phenol. In the photocatalysis process, light and photons are involved in the catalyst interaction, creating electron holes. For an efficient photocatalysis process, a semiconductor must have a suitable band gap, good photochemical stability, and high sunlight absorption coefficients [7-10]. One of the most excellent and unique photocatalysts is graphitic carbon nitride, g-C_3N_4 [11].

Graphitic carbon nitride (g-C_3N_4) is composed of triazine and heptazine or tri-s-triazine and has a suitable band gap for low-energy activation. It is also very stable, inexpensive, and non-toxic to the environment. However, g-C_3N_4 has its drawbacks, especially in photocatalytic activity reactions where it has a high recombination of charge carriers and a low specific surface area [12].

There are many ways to overcome the drawbacks of g-C_3N_4, including doping any metal elements towards it. Metal doping with g-C_3N_4 can improve photocatalytic activity by inhibiting and delaying the recombination of the photogenerated electron-hole pairs in the semiconductors [13]. In addition, the electron entrapment in the center of the metallic dope helps in the production of a highly oxidized hole. Furthermore, a lower band gap of doped g-C_3N_4 can also increase the longevity and mobility of the charge carriers [14]. Based on research by Zhao et al. [15], transition metals such as cobalt, copper, and iron can coordinate with the nitrogen pockets of some nitrogen-rich compounds, other than being a component of the catalyst. Doping metals like copper with g-C_3N_4 can help reduce the phenol since Cu/g-C_3N_4 has excellent electrocatalytic activity for oxygen reduction in the basic medium [16]. Other than that, copper is also affordable. It is one of the plentiful metals with an outstanding activation performance on the breakdown of contaminants over a wide pH range. Doping copper with g-C_3N_4 can increase the photocatalytic activity by increasing the g-C_3N_4's electron-hole separation efficiency [17]. Furthermore, doping g-C_3N_4 with copper can prevent the recombination of the photogenerated carrier by enhancing the copper's metal surface's electrons and increasing the formation of the active sites in the nitrogen-rich matrix [18]. The band gap can also be reduced by improving UV light absorption by increasing the amount of copper doped with g-C_3N_4 [19].

Therefore, this study focuses on copper-doped graphitic carbon nitride as a photocatalyst to degrade phenols under fluorescent and sunlight irradiation. This study utilized fluorescent and sunlight since sunlight is the most efficient and readily available renewable energy on earth. In contrast, UV light irradiation is a small part of the solar radiation, providing only 3-5% of the total.

METHODOLOGY

Synthesis

The chemicals used were melamine ($C_3H_6N_6$, 99%, Sigma-Aldrich), copper (II) nitrate (99%. $CuNO_3$, R&M Chemicals), phenol (99%, C_6H_5OH, R&M Chemicals), and deionized water. The pure g-C_3N_4 was prepared by the thermal decomposition of melamine and continued with the liquid exfoliation method according to a previous study with minor modifications [20]. The 20 g of melamine was placed in an alumina crucible and covered with a lid, and then heated at 3°C per minute with a heating rate of 2 hours in a muffle furnace. After switching off the heat, it was maintained at a temperature of 600°C for 2 hours. After cooling to room temperature, the pure g-C_3N_4 was dispersed in 100 mL of deionized water before being sonicated for about 5 hours. The product was centrifuged for 5 minutes at 3000 rpm before it was dried overnight and ground into fine powder. In addition, a series of g-C_3N_4 doping with copper was prepared by changing the mass of copper (II) nitrate. The weighed copper (II) nitrate was mixed with 30 mL of deionized water, and stirred until dissolved. Then, the dissolved copper (II) nitrate was added into 20 g of melamine powder and placed in an alumina crucible. The synthesis of copper-doped g-C_3N_4, (Cu/g-C_3N_4) was prepared using the same conditions as pure g-C_3N_4, except that the mass of the copper (II) nitrate was changed to 0.1 g, 0.2 g, 0.3 g, 0.4 g, and 0.5 g.

Characterization

The synthesized sample was characterized using Fourier-transform infrared spectroscopy, (FTIR), X-ray diffraction (XRD), Field-emission scanning electron microscopy (FESEM), and energy dispersive X-ray (EDX) analysis.

FTIR was utilized to study the functional group of the samples. For this analysis, the solid sample was mixed with potassium bromide, KBr at 1:100 ratio, and ground using a pestle and mortar. The mixture was then put in a mini-press to compress the KBr and photocatalyst mixture to form a thin and semi-transparent disk. FTIR spectra were recorded on a Perkin Elmer 100 FTIR Spectrometer using the Attenuated Total Reflectance (ATR) method in a range of 4000-500 cm^{-1}.

XRD was used to identify the crystalline of the pure g-C_3N_4 and Cu/g-C_3N_4. XRD patterns of the

samples were obtained via an X-Ray diffractometer, Bruker/ D8 advanced, XRD operating at 40 kV, 30 mA and Cu Kα radiation (λ = 1.5406 nm) at 2θ = 10°–90°.

The surface morphology of pure g-C_3N_4 and Cu/g-C_3N_4 was investigated by FESEM (Crossbeam 340 Zeiss FESEM). Meanwhile, the elements weight percentage of the sample surface was investigated via the energy dispersive X-ray (EDX) analysis. Each sample was scanned using the following parameters: 15.0 kV accelerating voltage, 2.56160 nA probe current, and a 0-20 keV energy range.

Photocatalytic Activity

The photocatalytic activity of pure g-C_3N_4 and Cu/g-C_3N_4 was evaluated by the degradation of phenol under visible light (fluorescent) and sunlight irradiation, and analyzed by UV-Vis Spectrophotometer. The photocatalytic process under fluorescent irradiation was carried out in the photoreactor equipped with four quartz tube reactors. Fluorescent light source was 300 W Xe lamp with a cut-off filter of less than 400 nm.

The 10 mg of catalyst was added into 20 mL of 10 ppm phenol solution. Then, the suspensions were magnetically stirred for 30 minutes in the dark for phenol adsorption. After that, the suspension was irradiated under fluorescent or sunlight irradiations. The temperature was maintained at 20°C with a circulating air system in the photoreactor.

After the irradiation, the suspensions were then collected, centrifuged, and analyzed by UV-Vis spectrophotometer, where the wavelength was detected at 275 nm. The degradation efficiency (E_t) of phenol was evaluated using the following equation [21]:

$$E_t = (1-C_t/C_0) \times 100\% \quad (1)$$

where C_0 denotes the phenol concentration at the time t=0 and C_t denoting the concentration of phenol at the time, t.

The kinetics reaction of phenol degradation was analyzed by the pseudo-first-order kinetics using the following equation [21]:

$$\ln (1-C_t/C_0) = -kt \quad (2)$$

Where C_0 and C_t denote phenol concentration at the time, t=0, t and k denoting the rate constant.

RESULTS AND DISCUSSION

Characterization

The pure graphitic carbon nitride g-C_3N_4 and copper doped g-C_3N_4 were synthesized using the hydrothermal of melamine and copper (II) nitrate. The synthesized sample was characterized by using FTIR, XRD, FESEM, and EDX.

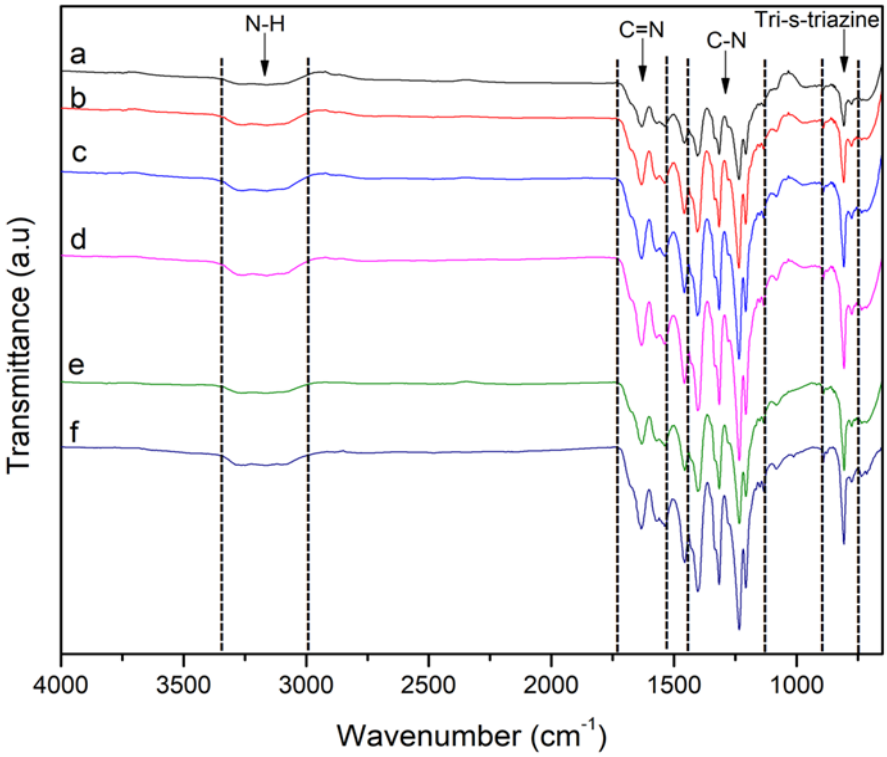

Figure 1. FTIR for (a) g-C_3N_4, (b) 0.1Cu/g-C_3N_4, (c) 0.2Cu/g-C_3N_4, (d) 0.3Cu/g-C_3N_4, (e) 0.4Cu/g-C_3N_4, (f) 0.5Cu/g-C_3N_4

Table 1. The summaries of significant peak of g-C_3N_4

Vibration	Wavenumber (cm^{-1})	Wavenumber (cm^{-1}) from references	References
N-H	3249.26	3000-3400	[17, 22, 23]
C-N Stretching	1403.45 1456.11 1315.19 1233.80	1411 1461 1311 1234	
C=N heterocycles	1622.74 1538.31	1627 1539	
Tri-s- triazine structure	807.09	806	

Figure 1 shows the IR spectrum for pure g-C_3N_4 and Cu/g-C_3N_4, with different masses of copper doped with g-C_3N_4. Based on the IR spectrum g-C_3N_4, the broadband at 3249.26 cm^{-1} indicates the N-H stretching with the interaction of the O-H absorbed H_2O [17, 22]. In addition, the absorption peaks at 1633.74, 1538.31, 1403.45, 1315.19, and 1223.80 cm^{-1} indicate the heterocycles of the carbon nitride [17, 22, 23]. The sharp absorption peak at 807.09 cm^{-1} indicates the absorption of the tri-s-triazine ring structure [17, 22]. Hence, it can be concluded that the g-C_3N_4 was successfully synthesized, as reported previously [17, 22, 23]. Moreover, the IR spectrum also shows their similarity in the absorption features, which also indicates that the doping of g-C_3N_4 with different amounts of copper has a basic structure which is the same as pure g-C_3N_4 and successfully synthesized [17].

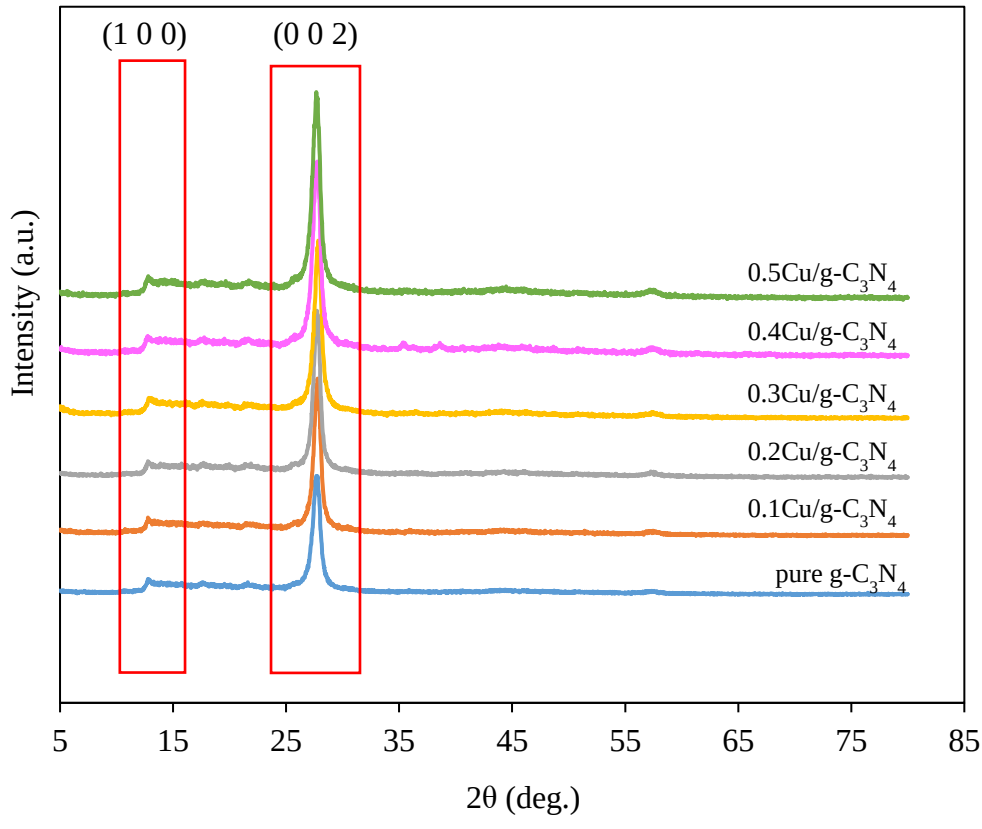

Figure 2. XRD patterns of pure g-C_3N_4, 0.1Cu/g-C_3N_4, 0.2Cu/g-C_3N_4, 0.3Cu/g-C_3N_4, 0.4Cu/g-C_3N_4, and 0.5Cu/g-C_3N_4

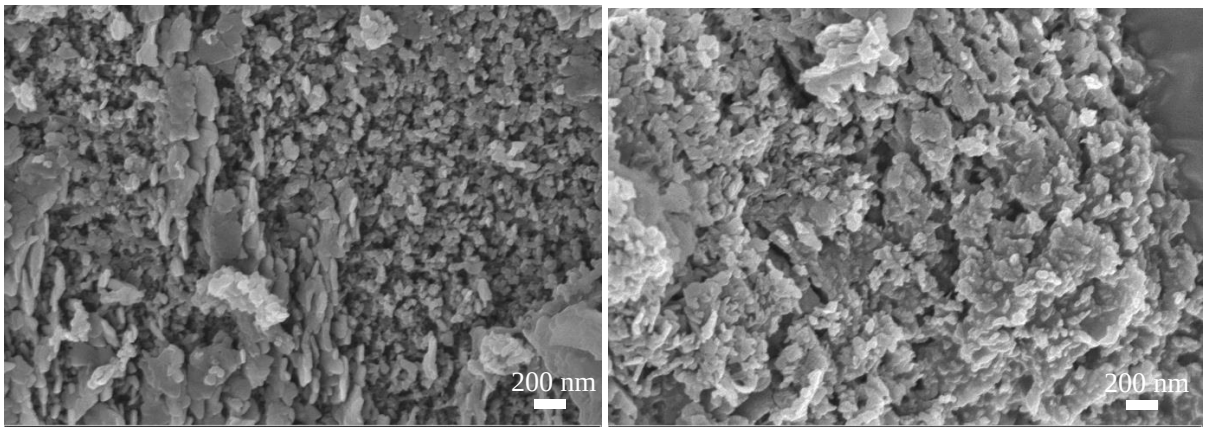

Figure 3. a) FESEM results for pure g-C_3N_4, and (b) FESEM results for 0.5Cu/g-C_3N_4

Tabel 2. Elemental analysis of synthesized samples by EDX.

	w (%)		
Sample	**N**	C	**Cu**
Pure g-C_3N_4	51.9	48.1	0
0.5Cu/g-C_3N_4	54.2	44.6	1.3

The XRD patterns of pure g-C_3N_4 and Cu/g-C_3N_4 with different masses of copper are shown in Figure 2. The XRD patterns show a weak diffraction peak at 12.8° and a stronger one at 28.4°. The diffraction peak at 12.8° was attributed to the (100) peak of the in-plane structural pattern of tri-s-triazine units [24]. The peak at 28.4° was attributed to the interlayer stacking of the conjugated aromatic ring, identified as the (002) peak of g-C_3N_4 [24]. The peak of Cu/g-C_3N_4 with different masses of copper has a pattern that matches the pure g-C_3N_4, with a slight decrease in the intensity of diffraction at the weak peaks. The XRD pattern also shows that the structure of g-C_3N_4 does not change even when doped with copper, and that all of them have similar structures [25].

Figure 3 shows the surface morphologies of the pure g-C_3N_4 and 0.5Cu/g-C_3N_4, which were captured by FESEM. It shows that the size particles of 0.5Cu/g-C_3N_4 become more aggregated compared to the pure g-C_3N_4 after copper was introduced on the surface of the g-C_3N_4 [17].

Table 2 shows the elemental analysis by EDX analysis, which proves that the elements present were N, C, and Cu. Based on the EDX findings, there was 1.3% Cu in 0.5Cu/g-C_3N_4, which concludes that Cu was successfully doped into the g-C_3N_4 structure compared to the pure g-C_3N_4.

Photocatalytic Degradation Studies

The photocatalytic degradation of phenol solution was studied with puree g-C_3N_4, and the different amounts of copper doped with g-C_3N_4 ranged from 0.1g to 0.5g in their mass. Three conditions were tested namely dark, fluorescent irradiation, and under sunlight for 5 to 120 minutes. The residual was analyzed using UV-Vis Spectroscopy with 275 nm as the maximum absorption wavelength for phenol.

Figure 4 shows the degradation efficiency of pure g-C_3N_4, 0.1Cu/g-C_3N_4, 0.2Cu/g-C_3N_4, 0.3Cu/g-C_3N_4, 0.4Cu/g-C_3N_4, and 0.5Cu/g-C_3N_4 for phenol degradation under fluorescent irradiation. The higher the C/C_0 values, the lower the efficiency of degradation. From the figure, it can be seen that all the photocatalysts have poor degradation efficiency under dark conditions, as their C/C_0 value is high. Moreover, there was also a fluctuating trend indicating the occurrence of adsorption/desorption during the darkness. Meanwhile, Cu/g-C_3N_4 shows the highest photocatalytic efficiency compared to pure g-C_3N_4 under fluorescent irradiation. The degradation efficiency of the 0.5Cu/g-C_3N_4 towards phenol at 120 minutes was 50.77%. Meanwhile the pure g-C_3N_4 shows the lowest degradation efficiency of 43.08%. This shows that phenol degradation is highly dependent on the degree of the copper doping with the g-C_3N_4, as the degradation efficiency increased with increasing copper doping from 0.1 g to 0.5 g under fluorescent light irradiation. A similar observation was made by Oliveros et al. [20], where the degradation efficiency increased with the amount of copper-doped with g-C_3N_4, implying that an increase in copper mass could provide more catalytic areas for the phenol degradation.

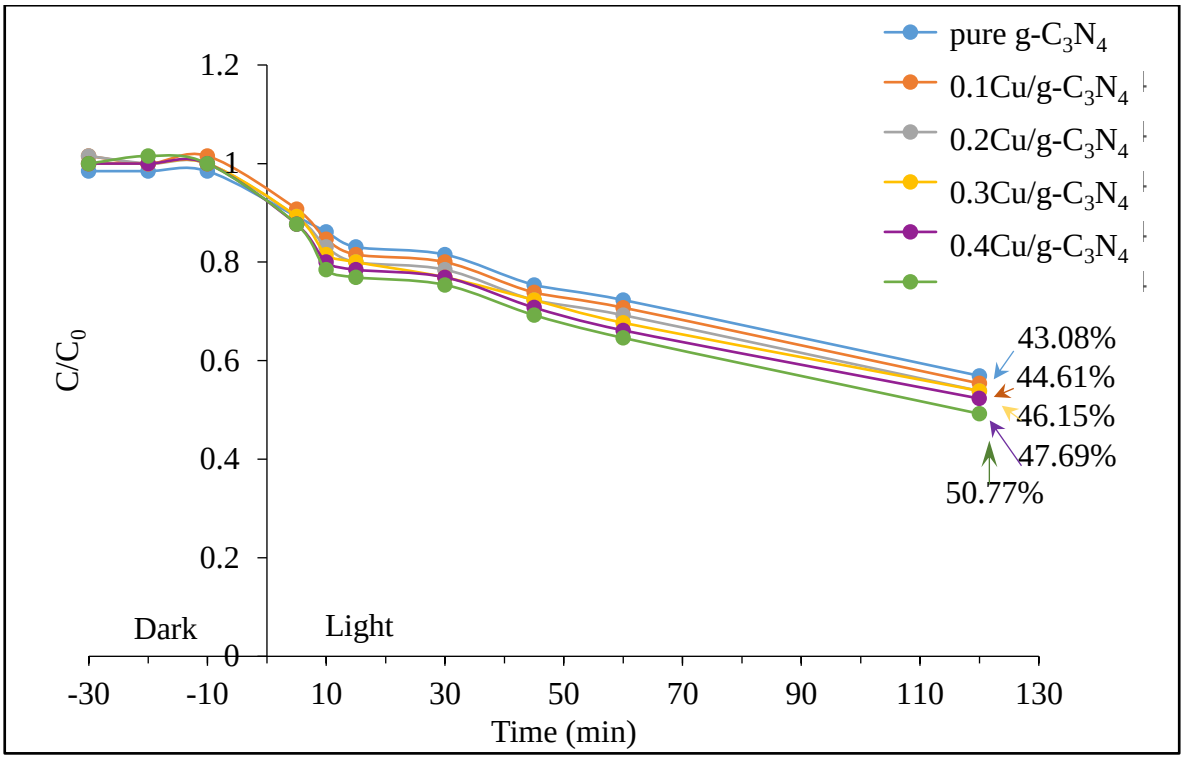

Figure 4. Photocatalytic degradation efficiency of pure g-C_3N_4, 0.1Cu/g-C_3N_4, 0.2Cu/g-C_3N_4, 0.3Cu/g-C_3N_4, 0.4Cu/g-C_3N_4, and 0.5Cu/g-C_3N_4 under fluorescent irradiation.

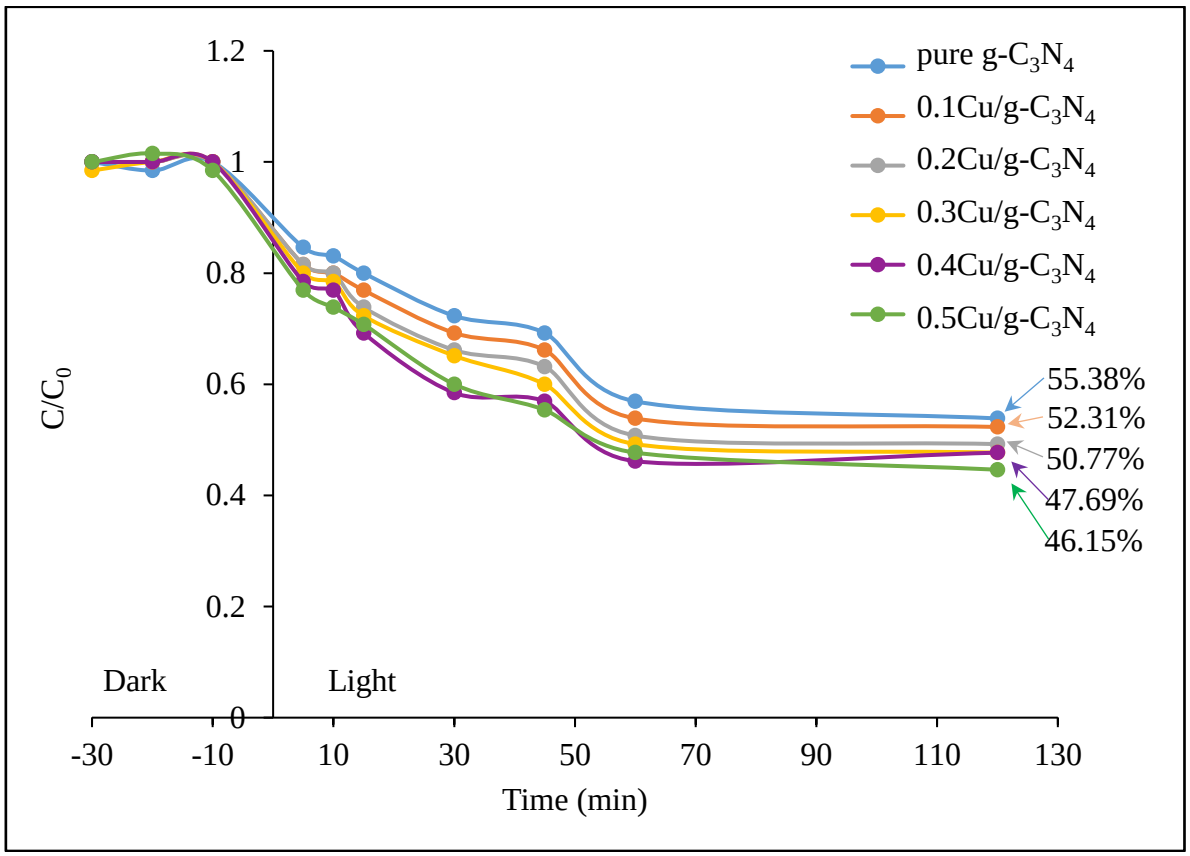

Figure 5. Photocatalytic degradation efficiency of pure g-C_3N_4, 0.1Cu/g-C_3N_4, 0.2Cu/g-C_3N_4, 0.3Cu/g-C_3N_4, 0.4Cu/g-C_3N_4, and 0.5Cu/g-C_3N_4 under sunlight irradiation.

Next, under sunlight irradiation, the photocatalysts also demonstrated low performance in their degradation under dark conditions since they have higher C/C_0. Pure g-C_3N_4 shows the lowest degradation efficiency (46.15%) towards phenol at 120 minutes compared to Cu/g-C_3N_4 under sunlight irradiation. Moreover, the degradation efficiencies of Cu/g-C_3N_4 increased with an increasing amount of copper, where 0.5Cu/g-C_3N_4 has the highest degradation efficiency (55.38%). These results show that the increased amount of copper doped with g-C_3N_4 improves photocatalytic performance and increases the production of photogenerated electrons and holes, thus increasing the efficiency of the photocatalysts [21]. In addition, an increase in time will also increase the photocatalysts' efficiency in terms of their percentage towards the degradation of phenol since higher hydroxyl radicals can be formed [22]. Under sunlight irradiation, the percentage of degradation efficiency was slightly higher compared to that under fluorescent irradiation because the sunlight itself efficiently helps the photocatalyst, especially Cu/g-C_3N_4, to further degrade the phenol as the sunlight power is higher than that of the fluorescent irradiation. According to Vukšić et al. [22], photocatalyst reaction occurs due to the irradiation of the sunlight right at the surface layer of the Cu/g-C_3N_4, where their photon energy can be activated.

Kinetic Analysis

In this study, the kinetic behavior of the photodegradation process was tested for each photocatalyst for 0 to 120 minutes under fluorescent irradiation [23]. Figure 6 reveals the plot of $-ln\ (1-C_t/C_0)$ vs time. The rate constant, k, was observed based on the pseudo-first-order rate with 0.5Cu/g-C_3N_4 showing the maximum degradation constant (0.0046 min^{-1}). Meanwhile, the pure g-C_3N_4 shows the minimum degradation constant for phenol at 0.0038 min^{-1}. For the rest of the photocatalysts, their degradation rate constant increased with an increasing amount of copper being doped with pure g-C_3N_4, namely 0.1Cu/g-C_3N_4, (0.0040 min^{-1}) and 0.2Cu/g-C_3N_4 (0.0041 min^{-1}). For 0.3Cu/g-C_3N_4 and 0.4Cu/g-C_3N_4, the degradation rate constant was 0.0040 min^{-1} and 0.0042 min^{-1}, respectively. Therefore, the rate constant order was 0.5Cu/g-C_3N_4 > 0.4Cu/g-C_3N_4 > 0.2Cu/g-C_3N_4 > 0.3Cu/g-C_3N_4 > 0.1Cu/g-C_3N_4 > pure g-C_3N_4.

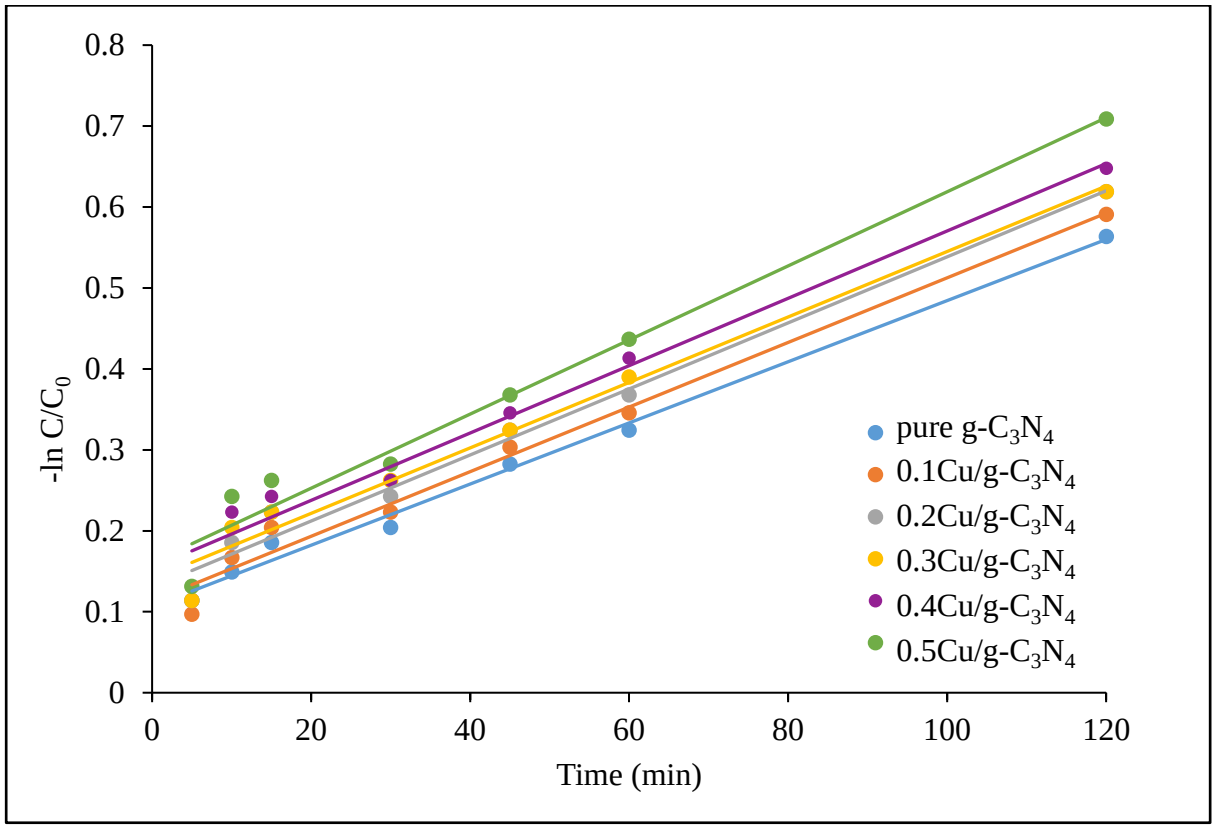

Figure 6. Pseudo first-order kinetic of pure g-C_3N_4, 0.1Cu/g-C_3N_4, 0.2Cu/g-C_3N_4, 0.3Cu/g-C_3N_4, 0.4Cu/g-C_3N_4, and 0.5Cu/g-C_3N_4 under fluorescent irradiation.

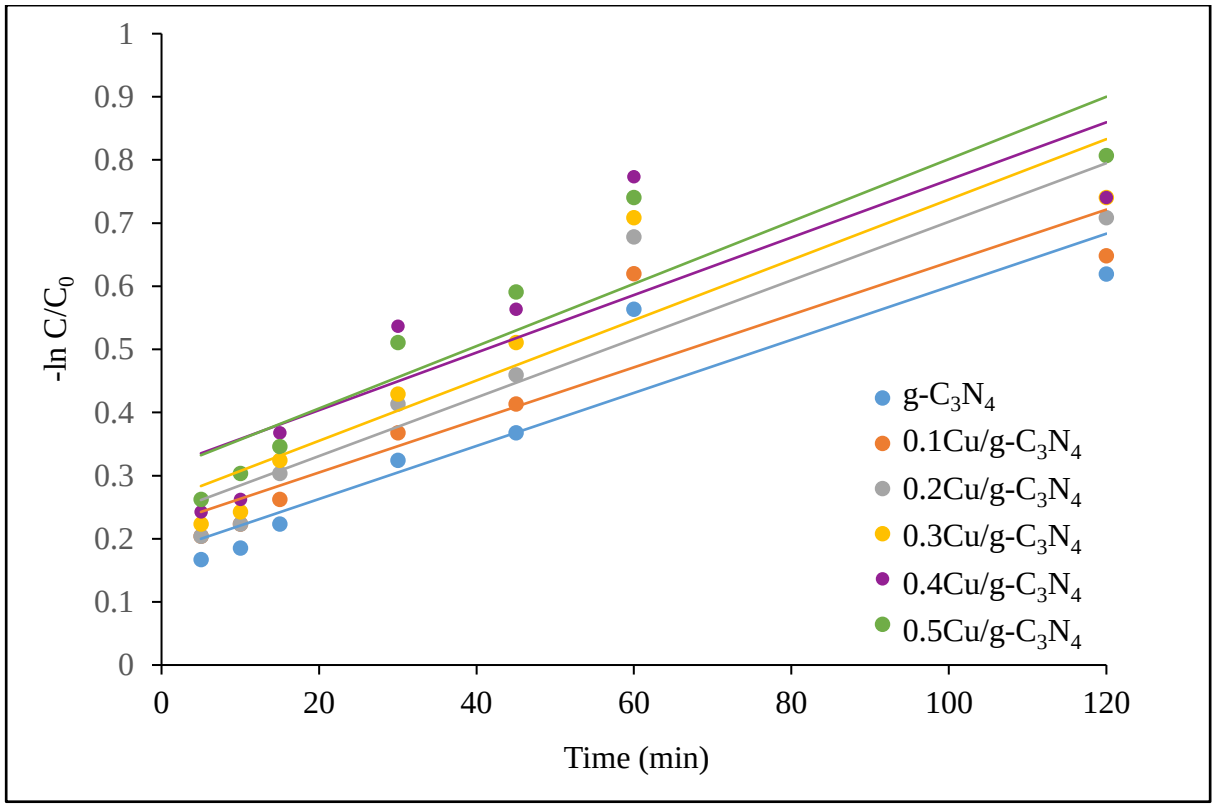

Figure 7. Pseudo first-order kinetic of pure g-C_3N_4, 0.1Cu/g-C_3N_4, 0.2Cu/g-C_3N_4, 0.3Cu/g-C_3N_4, 0.4Cu/g-C_3N_4, and 0.5Cu/g-C_3N_4 under sunlight irradiation.

The kinetic behavior of the photodegradation process was tested for each photocatalyst for 0 to 120 minutes under sunlight irradiation. Figure 7 shows the plot of $-ln\ (1-C_t/C_0)$ vs time under sunlight irradiation. This figure shows that 0.5Cu/g-C_3N_4 has the highest degradation rate constant, k (0.0049 min^{-1}). Meanwhile, pure g-C_3N_4 shows the minimum degradation constant for phenol at 0.0042 min^{-1}. For the rest of the photocatalysts, their degradation rate constant increased with an increasing amount of copper being doped with g-C_3N_4 namely 0.1Cu/g-C_3N_4 at 0.0042 min^{-1} and 0.2Cu/g-C_3N_4 at 0.0046 min^{-1}. For 0.3Cu/g-C_3N_4 and 0.4Cu/g-C_3N_4, the degradation rate constant was 0.0048 min^{-1} and 0.0046 min^{-1}, respectively. Therefore, the rate constant order was 0.5Cu/g-C_3N_4 > 0.3Cu/g-C_3N_4 > 0.4Cu/g-C_3N_4 > 0.2Cu/g-C_3N_4 > 0.1Cu/g-C_3N_4 > pure g-C_3N_4.

Table 3 below shows the detection of the kinetic parameters based on the pseudo-first-order kinetic analysis for the different types of photocatalysts in the degradation of phenol during a contact time of 2 hours at an initial concentration of 10 ppm. Table 3 shows the degradation of phenol under fluorescent light. It can be seen that 0.5Cu/g-C_3N_4 with a degradation percentage of 50.77% has the highest rate constant, k (0.0049 min^{-1}) and the shortest half-life (2.51 hours) compared to the other photocatalysts. The rate constant, k of 0.3Cu/g-C_3N_4 and 0.4Cu/g-C_3N_4 was lower than the 0.5Cu/g-C_3N_4 at 0.0040 min^{-1} and 0.0042 min^{-1}, respectively, which was lower than 0.5Cu/g-C_3N_4. From the value of the rate constant k, 0.3Cu/g-C_3N_4 and 0.4Cu/g-C_3N_4 showed slower reactions compared to the other photocatalysts. The comparison with the degradation of phenol by TiO_2/AC in previous studies shows that the photocatalyst achieves 93.4% of the percentage degradation with a rate constant of, k (0.0037 min^{-1}) under fluorescent light irradiation.

Table 4 below shows the detection of the kinetic parameters based on the pseudo-first-order kinetic analysis for the different types of photocatalysts in the phenol degradation during a contact time of 2 hours at an initial concentration of 10ppm. Table 3 shows the degradation of phenol under sunlight irradiation. Here, it can be seen that 0.5Cu/g-C_3N_4 with a degradation percentage of 55.38% has the highest rate constant, k (0.0049 min^{-1}) and the shortest half-life (2.36 hours) compared to the other photocatalysts. Meanwhile, compared to another photocatalyst, such as Sn_3O_4 in the degradation of phenol, the photocatalyst achieved 65% in degradation with a rate constant, k of (0.0005 min^{-1}) under sunlight irradiation. To conclude, the kinetic study is important to determine the dynamics in terms of the adsorption process of the contaminants from the wastewater. These kinetic findings show the potential of the photocatalyst to degrade phenol under both conditions namely fluorescent and sunlight irradiation.

Table 3. Kinetic parameters (pseudo-first order) of Cu/g-C_3N_4 under fluorescent light irradiation in degrading phenol.

Type of Photocatalyst	R^2	k (min^{-1})	$t_{1/2}$ (h)	Degradation (%)	References
Pure g-C_3N_4	0.9926	0.0038	3.03	43.08	This study
0.1Cu/g-C_3N_4	0.9826	0.0040	2.89	44.61	
0.2Cu/g-C_3N_4	0.9828	0.0041	2.83	46.15	
0.3Cu/g-C_3N_4	0.9796	0.0040	2.89	44.61	
0.4Cu/g-C_3N_4	0.9782	0.0042	2.75	47.69	
0.5Cu/g-C_3N_4	0.9742	0.0046	2.51	50.77	
TiO_2/AC	0.6308	0.0037	Not mention	93.40	[24]

Table 4. Kinetic parameters (pseudo-first order) of Cu/g-C_3N_4 under sunlight irradiation in degrading phenol.

Type of Photocatalyst	R^2	k(min^{-1})	$t_{1/2}$ (h)	Degradation (%)	References
Pure g-C_3N_4	0.8736	0.0042	2.75	46.15	This study
0.1Cu/g-C_3N_4	0.8422	0.0042	2.75	47.69	
0.2Cu/g-C_3N_4	0.8322	0.0046	2.51	50.77	
0.3Cu/g-C_3N_4	0.8312	0.0048	2.40	52.31	
0.4Cu/g-C_3N_4	0.7232	0.0046	2.51	52.31	
0.5Cu/g-C_3N_4	0.8452	0.0049	2.36	55.38	
TiO_2/AC	0.9841	0.005	Not mention	65.00	[25]

CONCLUSION

In summary, copper-doped graphitic carbon nitride with different amounts of copper was successfully synthesized and characterized. The pure g-C_3N_4 and copper-doped g-C_3N_4 from 0.1Cu/g-C_3N_4 until 0.5Cu/g-C_3N_4 were characterized by FTIR, XRD, FESEM, and EDX. The FTIR results show that the pure g-C_3N_4 and copper-doped g-C_3N_4 were successfully synthesized since the functional groups of g-C_3N_4 were present in the IR spectra. The FTIR confirmed the presence of all vibration peaks of g-C_3N_4. The XRD patterns show that the copper-doped has no significant influence on the structure of pure g-C_3N_4, while the EDX analysis shows the presence of copper in g-C_3N_4. Based on the photocatalysts that were synthesized, 0.5Cu/g-C_3N_4 presented the highest degradation of phenol under visible irradiation for both conditions namely under fluorescent light and sunlight irradiation. The degradation efficiencies of phenol using 0.5Cu/g-C_3N_4 under fluorescent light irradiation was 50.76%, while under sunlight light irradiation, it was 55.38% for 120 minutes. The rate constant and half-life of the photocatalyst were determined using the pseudo-first-order rate law with $0.0046min^{-1}$ at 2.51 hours in their half-life under fluorescent light irradiation and $0.0049min^{-1}$ at 2.36 hours in their half-life under sunlight irradiation. This study revealed the potential of Cu/g-C_3N_4 as one of the highly active photocatalysts that can degrade phenol in the presence of visible light. The result of this study is in line with the Malaysian government's 12th Malaysia Plan to provide clean water and sanitization and contribute to achieving the Sustainable Development Goal (SDG6) of improving water quality by reducing pollution by 2030.

ACKNOWLEDGEMENTS

This research was supported in part with Kurita Asia Research Grant (23Pmy257) under file number 100-TNCPI/INT 16/6/2 (044/2023) provided by the Kurita Water and Environment Foundation. Furthermore, the authors gratefully acknowledge Universiti Teknologi MARA under Research Grant MyRA (600-RMC/GPM LPHD 5/3 (057/2021).

AUTHOR CONTRIBUTION

Nurul Izzah Norhisan – data curation, writing; Nur Nazzatul Azzin Ahmad Tarmizi data curation, writing; Salman Al Faridzy Akbar – data curation; Siti Hajar Alias – conceptualization, supervision, writing; Siti Nor Atika Baharin – review, editing; Sheikh Ahmad Izaddin Sheikh Mohd Ghazali – review, editing; and Hadi Nur – conceptualization, review, editing.

CONFLICT OF INTEREST

Authors declare no conflict of interest.

REFERENCES

1. Issakhov, A., Alimbek, A. and Zhandaulet, Y. (2021) The assessment of water pollution by chemical reaction products from the activities of industrial facilities: Numerical study. *Journal of Cleaner Production*, **282**, 1–23.

2. Kafle, B. P. (2020) Application of UV–VIS spectrophotometry for chemical analysis. In: Chemical Analysis and Material Characterization by Spectrophotometry. *Elsevier*.

3. Mei, H., Deng, L., Xie, J., Li, X., Wu, N., Hu, L., Huang, G., Mo, F., Chen, D., Xiao, H. and Yang, P. (2023) Co-exposure to phenols and phthalates during pregnancy with the difference of body size in twins at one month old. *Chemosphere*, **311**, 1–10.

4. Ismanto, A., Hadibarata, T., Kristanti, R. A., Maslukah, L., Safinatunnajah, N. and Kusumastuti, W. (2022) Endocrine disrupting chemicals (EDCs) in environmental matrices: Occurrence, fate, health impact, physio-chemical and bioremediation technology. *Environmental Pollution*, **302**, 1–15.

5. Wu, L., Ali, D. C., Liu, P., Peng, C., Zhai, J., Wang, Y. and Ye, B. (2018) Degradation of phenol via ortho-pathway by Kocuria sp. strain TIBETAN4 isolated from the soils around Qinghai Lake in China. *PLoS ONE*, **13(6)**, 1–10.

6. Ameta, R., Solanki, M. S., Benjamin, S. and Ameta, S. C. (2018) Photocatalysis. In: Advanced Oxidation Processes for Wastewater Treatment: Emerging Green Chemical Technology. *Elsevier Inc.*, **1**, 35–75.

7. Alias, S. H., Mohamed, N., Loon, W. and Chandren, S. (2019) Synthesis of carbon self-doped titanium dioxide and its activity in the photocatalytic oxidation of styrene under visible light irradiation. *Malaysian Journal of Fundamental and Applied Sciences*, **15**, 291–297.

8. Ibrahim, N. S., Leaw, W. L., Mohamad, D., Alias, S. H. and Nur, H. (2020) A critical review of metal-doped TiO_2 and its structure–physical properties–photocatalytic activity relationship in hydrogen production. *International Journal of Hydrogen Energy*, **45**, 28553–28565.

9. Sheikhnejad-bishe, O., Zhao, F., Rajabtabar-darvishi, A. and Khodadad, E. (2014) Influence of temperature and surfactant on the photocatalytic performance of TiO_2 Nanoparticles. *International Journal of Electrochemical Science*, **9**, 4230–4240.

10. Sheikh Mohd Ghazali, S. A. I., Fatimah, I., Zamil, Z. N., Zulkifli, N. N. and Adam, N. (2023) Graphene quantum dots: A comprehensive overview. *De Gruyter Open Ltd.*, **1**, 21–22.

11. Tahir, M. B., Iqbal, T., Rafique, M., Rafique, M. S., Nawaz, T. and Sagir, M. (2020) Nanomaterials for photocatalysis. In: Nanotechnology and Photocatalysis for Environmental Applications. *Elsevier*, **1**, 65–76.

12. Ajiboye, T. O., Kuvarega, A. T. and Onwudiwe, D. C. (2020) Graphitic carbon nitride-based catalysts and their applications: A review. *Nano-Structures and Nano-Objects*, **24**, 1–23.

13. Sakuna, P., Ketwong, P., Ohtani, B., Trakulmututa, J., Kobkeatthawin, T., Luengnaruemitchai, A. and Smith, S. M. (2022) The Influence of Metal-Doped Graphitic Carbon Nitride on Photocatalytic Conversion of Acetic Acid to Carbon Dioxide. *Frontiers in Chemistry*, **10**, 1–12.

14. Palani, G., Apsari, R., Hanafiah, M. M., Venkateswarlu, K., Lakkaboyana, S. K., Kannan, K., Shivanna, A. T., Idris, A. M. and Yadav, C. H. (2022) Metal-Doped Graphitic Carbon Nitride Nanomaterials for Photocatalytic Environmental Applications-A Review. *Nanomaterials*, **12**, 1–14.

15. Zhao, Y., Chu, Y., Ju, X., Zhao, J., Kong, L. and Zhang, Y. (2018) Carbon-supported copper-based nitrogen-containing supramolecule as an efficient oxygen reduction reaction catalyst in neutral medium. *Catalysts*, **8(53)**, 1–16.

16. Nisha, V., Moolayadukkam, S., Paravannoor, A., Panoth, D., Chang, Y. H., Palantavida, S., Hinder, S. J., Pillai, S. C. and Vijayan, B. K. (2022) Cu doped graphitic C_3N_4 for p-nitrophenol reduction and sensing applications. *Inorganic Chemistry Communications*, **142**, 1–10.

17. Liu, K., Wang, X., Li, C., Gao, M., Cao, N., Zhao, X., Li, W., Ding, X., Li, Z., Du, X., Feng, J., Ren, Y., Wei, T. and Zhang, M. (2022) Facile fabrication metal Cu-decorated g-C_3N_4 photocatalyst with Schottky barrier for efficient pollutant elimination. *Diamond and Related Materials*, **126**, 1–11.

18. Hu, S., Qu, X., Li, P., Wang, F., Li, Q., Song, L., Zhao, Y. and Kang, X. (2018) Photocatalytic oxygen reduction to hydrogen peroxide over copper doped graphitic carbon nitride hollow microsphere: The effect of Cu(I)-N active sites. *Chemical Engineering Journal*, **334**, 410–418.

19. Li, X. and Gan, X. (2022) Photo-Fenton degradation of multiple pharmaceuticals at low concentrations via Cu-doped-graphitic carbon nitride (g-C_3N_4) under simulated solar irradiation at a wide pH range. *Journal of Environmental Chemical Engineering*, **10**, 1–11.

20. Oliveros, A. N., Pimentel, J. A. I., de Luna, M. D. G., Garcia-Segura, S., Abarca, R. R. M. and Doong, R. A. (2021) Visible-light photocatalytic diclofenac removal by tunable vanadium pentoxide/ boron-doped graphitic carbon nitride composite. *Chemical Engineering Journal*, **403**, 1–12.

21. Mohammed, R. and Ali, M. E. M. (2023) Decorated ZnO nanorods with Bi_2S_3 nanosheets for enhanced photocatalytic removal of antibiotics and analgesics: Degradation mechanism and pathway. *Environmental Nanotechnology, Monitoring and Management*, **20**, 1–22.

22. Vukšić, M., Kocijan, M., Ćurković, L., Radošević, T., Vengust, D. and Podlogar, M. (2022) Photocatalytic Properties of Immobilised Graphitic Carbon Nitride on the Alumina Substrate. *Applied Sciences*, **12**, 1–13.

23. Narkbuakaew, T. and Sujaridworakun, P. (2020) Synthesis of Tri-S-Triazine Based g-C_3N_4 Photocatalyst for Cationic Rhodamine B Degradation under Visible Light. *Topics in Catalysis*, **63**,1086–1096.

24. Hasija, V., Sudhaik, A., Raizada, P., Hosseini-Bandegharaei, A. and Singh, P. (2019) Carbon quantum dots supported AgI /ZnO/phosphorus doped graphitic carbon nitride as Z-scheme photocatalyst for efficient photodegradation of 2, 4-dinitrophenol. *Journal of Environmental Chemical Engineering*, **7**, 1–12.

25. Zou, X., Silva, R., Goswami, A. and Asefa, T. (2015) Cu-doped carbon nitride: Bio-inspired synthesis of H_2-evolving electrocatalysts using graphitic carbon nitride (g-C_3N_4) as a host material. *Applied Surface Science*, **357**, 221–228.